

Identification and compensation of friction and force ripple in PMSLM based on the time-domain analysis of relay feedback

475

Xiang Zhang, Fuzhao Chen and Qian Chen
*China Academy of Railway Sciences Corporation Limited,
Locomotive and Car Research Institute, Beijing, China*

Yongjing Ma
*CRRC Changchun Railway Vehicles Co., Ltd., CRRC Corporation Limited,
Beijing, China*

Xiuwei Tong
*Brake Development Department,
Beijing Zongheng Electromechanical Technology Co., Ltd.,
China Academy of Railway Sciences Corporation Limited, Beijing, China, and*

Zhenhong Wang
CRRC Tangshan Co., Ltd., CRRC Corporation Limited, Beijing, China

Received 5 May 2025
Revised 11 June 2025
Accepted 13 June 2025

Abstract

Purpose – This study aims to propose a novel identification method to accurately estimate linear and nonlinear dynamics in permanent magnet synchronous linear motor (PMSLM) based on the time-domain analysis of relay feedback.

Design/methodology/approach – A mathematical model of the PMSLM-based servo-mechanical system was first established, incorporating the aforementioned nonlinearities. The model's velocity response was derived by analyzing its behavior as a first-order system under arbitrary input. To induce oscillatory dynamics, an ideal relay with artificially introduced dead-time components was then integrated into the servo-mechanism. Depending on the oscillations and the time-domain analysis, nonlinear formulas were deduced according to the velocity response of the servo-mechanism. Afterwards, the unknown model parameters can be solved on account of the cost function which utilizes the discrepancy between nominal position characteristics and temporary position characteristics, both of which are extracted from the oscillations. The proposed recognition method was validated through a two-stage process: (1) numerical simulation and calculation, followed by (2) real-time experimental verification on a direct-drive servo platform. Subsequently, leveraging the identification results, a novel control strategy was developed and its tracking performance was benchmarked against conventional control schemes.

Findings – Simulation results demonstrate that the proposed method achieves estimation accuracy within 8%. Building on this, a novel control strategy is developed by incorporating both friction pulsation and force pulsation identification results into the feedforward compensator. Comparative experiments reveal that this strategy significantly enhances tracking and positioning performance over traditional control schemes. In a word, this new identification method can be used in different process control and servo control systems. Moreover, parameter auto-tuning, feed forward compensation or disturbance observer can be investigated based on the obtained information to improve the system stability and control accuracy.

Originality/value – It is of great significance for the performance improvement of rail transit motor control equipment, such as electro-mechanical braking systems. By enhancing the efficiency of motor control, the performance of the product will be more outstanding.

Keywords Motor control, PMSLM, Relay feedback, Force ripple, Friction, Relay parameters

Paper type Technical paper

© Xiang Zhang, Fuzhao Chen, Qian Chen, Yongjing Ma, Xiuwei Tong and Zhenhong Wang. Published in *Railway Sciences*. Published by Emerald Publishing Limited. This article is published under the Creative Commons Attribution (CC BY 4.0) licence. Anyone may reproduce, distribute, translate and create derivative works of this article (for both commercial and non-commercial purposes), subject to full attribution to the original publication and authors. The full terms of this licence may be seen at [Link to the terms of the CC BY 4.0 licence](#).



1. Introduction

Motor control has been widely applied in the field of industrial control, and the rail transit industry is also increasingly applying motor control technology (Dong, Chen, Wang, Jia, & Man, 2020; Ye *et al.*, 2022; Zhao *et al.*, 2025). For instance, the newly proposed concept of all-electric drive train technology in recent years adopts motor control to replace traditional pneumatic control. Among them, the electro-mechanical braking system technology is currently a hot spot in the development of the braking industry (Chen *et al.*, 2024). A motor control strategy with high response and high precision is a necessary guarantee for the performance improvement of the electro-mechanical braking system.

Permanent magnet synchronous linear motor (PMSLM) is a type of motor control technology. The working principle of PMSLM is based on the interaction between electromagnetic force and permanent magnet. After the stator coil is energized, the magnetic field generated interacts with the permanent magnet on the mover to generate thrust, which makes the mover move along a straight track. Compared with traditional rotating machines, PMSLM not only has fast response and precise control, but also can reduce energy conversion loss and make energy conversion more efficient. In addition, low running noise is also its advantage. It combines the characteristics of permanent magnet motors and synchronous motors and can provide high-efficiency and precise linear motion control (Kadhim, Rostami, & Sharifian, 2024; Liu, Yao, & Jia, 2024). Its advantages are high force density, high dynamic response and no requirement of indirect coupling mechanisms. In the meanwhile, PMSLM have overcome difficulties, such as low efficiency, large volume and low accuracy, which are caused by mechanical transmitting elements in traditional servo-mechanical systems. As a compromise, any external disturbance will directly act on the output terminal of PMSLM, which results in low tracking accuracy and significant nonlinear characteristics. As a prominent case, magnetic field distortion may lead to force ripple that includes cogging and reluctance forces, both of which show a periodic relationship with respect to the displacement of the translator and the stator (Wang & Wang, 2023). Many studies on motor structure designs and different control strategies have been conducted to suppress the force ripple (Ahandani, Abbasfam, & Kharrati, 2022). As to motor structure design, force ripple can be diminished to some extent by optimizing the arrangement of permanent magnets and the shape of coil frames in PMSLM, which may be costly and degrade other specifications. Therefore, applying special control strategies to compensating for the friction as well as force ripple and expediting the tracking response is a common solution in recent years (Ahmad, Hassan, Khan, & Lazoglu, 2020; Liu *et al.*, 2025; Song, Xu, Fan, Yang, & Duan, 2022).

In order to achieve precision motion control of PMSLM, considerable control schemes have been proposed to compensate for the friction and force ripple, such as adaptive feed forward control (Qiao, Du, Wang, & Yang, 2023; Wang *et al.*, 2020; Yang, Li, Wang, & Zhang, 2021), neural networks (Rigatos, Zervos, Abbaszadeh, Siano, & Siadimas, 2020; Wu *et al.*, 2024) and disturbance observers (Li *et al.*, 2023; Pang *et al.*, 2023). In particular, the above-mentioned compensation methods require exact mathematical model of the friction and force ripple as a precondition. Furthermore, the common drawback of some control algorithms that are compensated by online model identification is that it requires extended time to estimate parameters. Since frequency sweep can just identify linear dynamics of servo-mechanism, there is not a general and unified approach available for estimating parameters of nonlinear systems. In this paper, a novel method based on relay feedback with time-domain analysis was investigated to identify the Coulomb friction, force ripple together with the linear portion of the servo-mechanism.

Generally speaking, analytical models of servo-mechanical systems can be derived from the laws of physics which is not suitable for complex systems, or identified by frequency sweep which requires lots of experimental data and is restricted to linear models. However, in the relay feedback, no extra signal-generating apparatus is required, and the oscillation output data which can entirely reflect the internal characteristics of the nonlinear servo-mechanism should be recorded. Therefore, simplicity and efficiency are two main advantages of the relay feedback (Zhou, Hao, Zou, & Liu, 2024). Since Astrom has presented the method for

observing limit cycle oscillations in the control process by relay feedback in 1984 (Astrom & Hagglund, 1984; Strm & Hgglund, 1984), the relay feedback technologies are widely used in the field of process control. Initially, the technologies were mostly employed for model identification and parameters tuning in industrial process control. Along with parameters of the friction and force ripple in servo-mechanism obtained by means of the relay feedback technologies (Rehan, Boiko, & Zweiri, 2024; Visioli & Sanchez-Moreno, 2024), it is gradually expanded into servo control fields in recent years. To enhance identification accuracy, some efforts have been devoted to modifying relay components.

As presented in Hofreiter, Mouka, and Trnka (2023), Pal and Mudi (2022), Taha and Emadi (2021), Wang, Lv, Wu, Zhang, and Gao (2024), the relay feedback method has been evolved to increase the identification accuracy and obtain extended identification information. Additionally, an effective friction identification approach based on the dual-relay feedback configuration is presented for a typical low-velocity servo system (Chen, Fang, & Luo, 2014). Besides, as reported in Leea, Tana, Limb, and Doua (2015), a feed-forward \pm feedback control structure is proposed for precision motion control of a permanent magnet linear motor. However, the above-mentioned analysis method is based on the described function method whose identification results may be less accurate because this method imports approximation of nonlinearities which takes only the fundamental frequency into account and ignores the influence of harmonics. As a consequence, a time-domain approach using relay feedback was proposed for asymmetric servo system identification considering the Coulomb friction as the only nonlinearity. In this instance, analytical equations were derived according to the step-response and initial state. Hence, the analytical formulas of the model parameters were illustrated and calculated based on some special sampling points (Shi, Han, Wu, & Liu, 2019). However, this method is not available for direct drive feed system due to the existence of force ripple in PMSLM. This means that the velocity response is no longer step-response when the force ripple is taken into consideration and analytical expressions of the model parameters cannot be obtained.

To address the problem as mentioned, this paper mainly focuses on a novel identification method based on the relay feedback tests in time-domain. In Section 2.1, the mathematical model of the servo-mechanical system was established. Section 2.2 described the application of traditional relay components for exciting oscillations in the feedback loop. Furthermore, the analytical expressions of velocity response and selection of sampling points in relay feedback experiments were illustrated. Afterwards, details of the identification process on the basis of the velocity response, position response with various relay parameters were elaborated comprehensively in Section 2.3. Moreover, simulations were conducted to verify this method and investigate how oscillations were influenced by different relay gains in Section 3. In Section 4, laying the foundation of the identification results, a feed-forward control scheme was designed, and its tracking performances were compared with a traditional control strategy. Finally, conclusions were drawn.

2. Model and identification

2.1 System model

Considering a general model of PMSLM, the servo-mechanical system which combines the mechanical dynamics and electrical dynamics can be represented

$$u(t) = K_e \dot{x} + R_i(t) + I \frac{di(t)}{dt} \quad (1)$$

$$f(f) = K_f i(t) \quad (2)$$

$$f(t) = m\ddot{x}(t) + f_r + f_f + f_\Delta \quad (3)$$

Where $u(t)$ is the armature voltage, $i(t)$ is the thrust current and $f(t)$ is the developed force; $x(t)$ refers to the motor position; f_r denotes the ripple force of the linear motor; f_f is the friction force and f_Δ represents the other uncertain disturbances. Other parameters are described in Table 1.

The friction force f_f can be considered as a combination of Coulomb and viscous friction. The model of the friction can be expressed as follows:

$$f_f = f_c \operatorname{sgn}(\dot{x}) + f_v \dot{x} \tag{4}$$

where f_c is the minimal level of Coulomb friction, and f_v is viscous friction coefficient.

In view of the fact that force ripple is associated with the displacement between the stator and the translator of PMSLM, force ripple can be described by a standard sinusoidal function with phase shift θ .

$$f_r = C \sin(\Omega x + \theta) = C_1 \cos(\Omega x) + C_2 \sin(\Omega x) \tag{5}$$

According to the (2)–(5), the following simplified equivalent model is obtained:

$$m\ddot{x} + f_v \dot{x} = F' \tag{6}$$

$$F' = K_f i(t) - f_c \operatorname{sgn}(\dot{x}) - C_1 \cos(\Omega x) - C_2 \sin(\Omega x) \tag{7}$$

Thereafter, transfer function of the linear dynamic of the servo-mechanical system can be expressed as follows:

$$G(s) = \frac{X(s)}{F'(s)} = \frac{1}{ms^2 + f_v s} = \frac{b}{s + a} \cdot \frac{1}{s} \tag{8}$$

Set $a = f_v/m$, $b = 1/m$, then, terms a , b , f_c , C_1 and C_2 are the parameters required for identification in this paper.

2.2 Time-domain analysis of relay feedback

In this section, analysis of relay feedback in time-domain for nonlinear system was investigated to explore the relationship between the parameters to be identified and prior information such as relay parameters and system outputs. As shown in Figure 1, traditional relay apparatus along with reasonable parameters were taken to excite the oscillation in the nonlinear servo-mechanism. Particularly, considering that the oscillation could not be generated under too small relay gain or dead time, some details about the effect of various relay gains and dead times on identification accuracy will be investigated in simulation study.

Based on the traditional relay feedback, the input current $i(t)$, which is generated by an ideal relay apparatus $u(t)$ with an artificial dead time D , can produce the exciting signal of rectangular wave. Under the exciting signal, the nonlinear system can oscillate with stable

Table 1. Linear motor parameters

Parameters	Physical meaning	Units
m	Mass of moving part	kg
K_e	Back EMF	V/(m/s)
K_f	Force constant	N/A
R	Resistance	Ω
L	Armature inductance	mH
Parameters	Physical meaning	Units

Source(s): Authors' own work

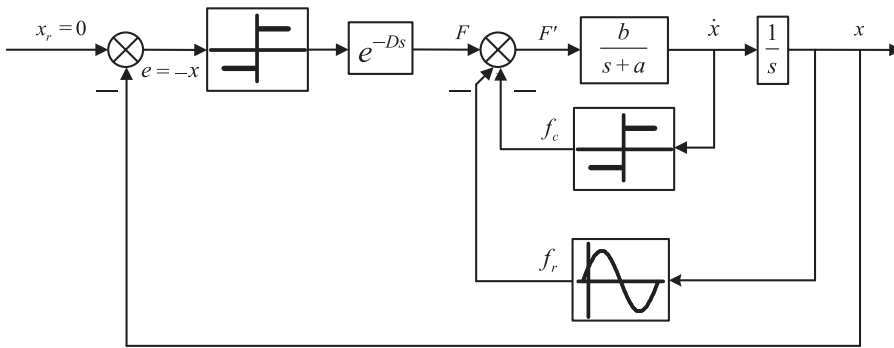


Figure 1. Block diagram of relay feedback for the nonlinear servo-mechanism. **Source(s):** Authors' own work

velocity response $v(t)$ and position response $x(t)$ as shown in [Figure 2](#). Combined with the block diagram as shown in [Figure 1](#), it can be concluded that the velocity response of the servo-mechanical system is equivalent to the response of a first-order system under arbitrary input. Moreover, similar to [Leea et al. \(2015\)](#), the form of the position response can be assumed as $e(t) = A\sin(\omega t) + B$, a standard sinusoidal with an offset. For convenience of analysis, the relay feedback process is segregated into two stages depending on the phase of the current input. Different from the relay feedback in time-domain as presented in [Shi et al. \(2019\)](#) which only takes the Coulomb and viscous friction into consideration, the force ripple is also considered because of the application of the PMSLM in servo-mechanism. Thus, the velocity response is no longer as simplicity as the step response due to the disturbance of the force ripple. As shown in [Figure 2](#), the disturbance of force ripple results in velocity fluctuation obviously.

The velocity response of the nonlinear system can be abstracted as an equivalent mathematical problem that the response of a first-order system under arbitrary input. Thereafter, the velocity response of the system can be expressed as follows:

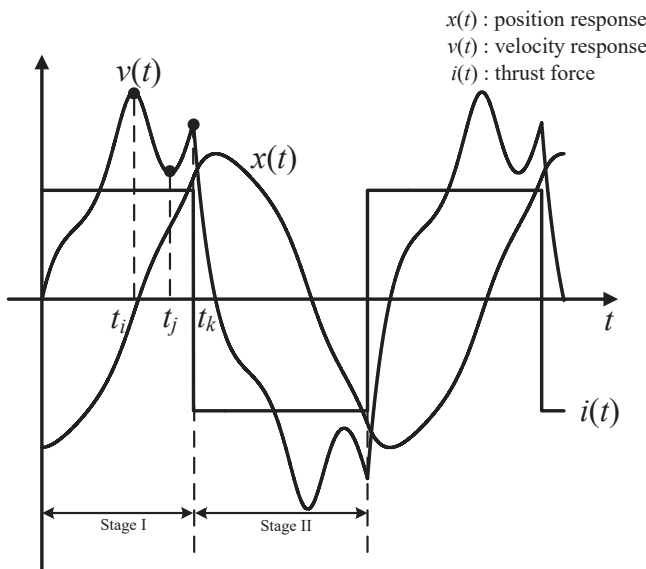


Figure 2. Oscillation in the nonlinear servo-mechanism. **Source(s):** Authors' own work

$$v(t) = \int_0^t h(\tau)g(t - \tau)d\tau \quad (9)$$

where $h(t)$ is the resultant force of thrust force, Coulomb friction and force ripple; $g(t)$ is the transfer function in time-domain obtained by inverse Laplace transformation. Considering discreteness of the sampling points, the velocity response can be discreted into (10).

$$v(t) = \sum_{i=0}^n h(t_i) \cdot \Delta t \cdot g(t - t_i) \quad (10)$$

where the Δt is the sampling period in simulation or real experiment. Accordingly, the discretization of the velocity response can be transferred into (11) according to the velocity of last moment.

$$y(t_i) = y(t_{i-1}) \cdot e^{-\frac{1}{\tau}\Delta t} + h(t_i) \cdot \Delta t \cdot b \cdot e^{-\frac{1}{\tau}(t_i - t_{i-1})} \quad (11)$$

where the system input $h(t_i)$ denotes the synthesis of thrust force, viscous friction and force ripple.

$$h(t_i) = \begin{cases} u(t_i) - f_c(t_i) + f_r(x(t_i)) & v(t_i) \geq 0 \\ -u(t_i) + f_c(t_i) + f_r(x(t_i)) & v(t_i) < 0 \end{cases} \quad (12)$$

Originally, in order to realize parameters identification, typical and essential sampling points as shown in Figure 2 should be extracted from the velocity response. Afterwards, analytical expressions can be obtained by substituting the velocity together with its corresponding position response. These formulas are presented in (13)–(15).

$$v(t_i) = v(t_{i-1}) \cdot e^{-\frac{1}{\tau}\Delta t} + h(t_i) \cdot \Delta t \cdot b \cdot e^{-\frac{1}{\tau}(t_i - t_{i-1})} \quad (13)$$

$$v(t_j) = v(t_{j-1}) \cdot e^{-\frac{1}{\tau}\Delta t} + h(t_j) \cdot \Delta t \cdot b \cdot e^{-\frac{1}{\tau}(t_j - t_{j-1})} \quad (14)$$

$$v(t_k) = v(t_{k-1}) \cdot e^{-\frac{1}{\tau}\Delta t} + h(t_k) \cdot \Delta t \cdot b \cdot e^{-\frac{1}{\tau}(t_k - t_{k-1})} \quad (15)$$

Since five parameters such as a , b , C_1 , C_2 and f_c are required to be identified, but there are only three formulas are available, a minimum of two sets of relay experiments should be performed with various relay parameters. However, in this case, not only the analytical expressions between the identified parameters and the relay parameters, but also the unique solution cannot be explicitly derived, since (13)–(15) are not linear equations. Theoretically, due to the nonlinear nature of the equations, it is essential to use additional characteristics of the oscillations to achieve the optimal solution by a numerical solving method.

2.3 Parameter identification based on genetic algorithm

Unlike traditional relay feedback approaches with approximation of nonlinear components in frequency domain, the time-domain analysis of the relay feedback process is accurate in formulas. However, as a trade-off, there are no analytical expressions for the identified parameters, and multiple solutions may satisfy the nonlinear formulas using numerical solving method. Thereafter, our motivation is to utilize additional characteristics of the stable oscillations excited by the appropriate relay gain and dead time to solve the identified model parameters. For this purpose, a numerical method is put forward by utilizing the nonlinear formulas and characteristics of the oscillations.

Originally, the position output, velocity output and the current input from the relay feedback loop can be measurable in this position feedback system. Based on the measurable position output, both the definition of nominal position characteristics (NPCs) and temporary position characteristics (TPCs) are introduced. As mentioned previously, the characteristics of position output contain offset (b), frequency (ω) and amplitude (A). Thus, the NPCs represent the characteristics of the position output generated by the given model in simulation or the practical servo-mechanism in relay feedback experiments, while the TPCs denote the characteristics of the position output excited by the temporary model parameters in numerical solving process. Subsequently, the cost function for parameters identification can be established as (16) depending on the discrepancy between the NPCs and TPCs.

$$J = \min_{\phi_i \in \Phi} \|I - B\Phi\|_2^2 \tag{16}$$

where $I = \begin{pmatrix} 1 \\ 1 \\ 1 \end{pmatrix}$, $B = \begin{pmatrix} A_0 & 0 & 0 \\ 0 & b_0 & 0 \\ 0 & 0 & \omega_0 \end{pmatrix}$, $\Phi = \begin{pmatrix} 1/A_i \\ 1/b_i \\ 1/\omega_i \end{pmatrix}$.

Note that A_0 , b_0 and ω_0 denotes the amplitude, offset and frequency of the NPCs, respectively. Meanwhile, note that Φ represents the amplitude, offset and frequency of the TPCs, whose oscillation is generated by substituting the intermediate model parameters into the solving process. To numerically solve the model parameters, genetic algorithm (GA) is implemented to find the optimal parameters by fitting the TPCs with the NPCs while taking an initial guess and a rational value range of the identified model parameters.

For further elaboration of the numerical solving method, the calculation flow chart is illustrated in Figure 3, and the details of the solving process are explained as follows:

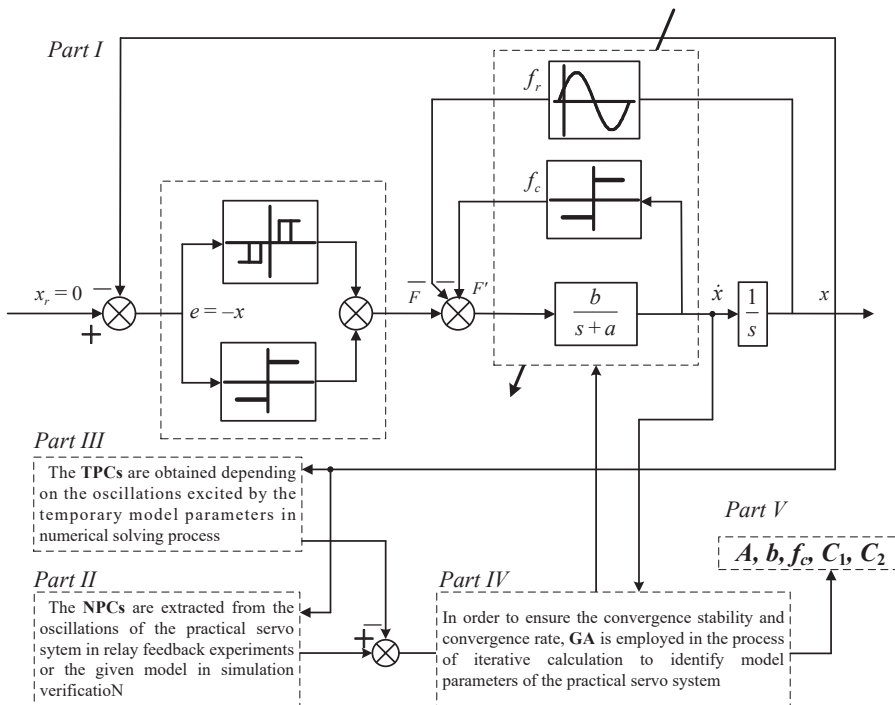


Figure 3. The flow chart of parameters identification. Source(s): Authors' own work

- (1) Oscillations of the nonlinear servo-mechanism can be excited by choosing reasonable relay parameters in position feedback loop.
- (2) The NPCs, which include frequency, offset and amplitude, are extracted from the oscillations of the practical servo-mechanical system in relay feedback experiments or the given model in simulation verification.
- (3) Current inputs, velocity outputs and its corresponding position outputs are sampled from the oscillations and substituted into the nonlinear formulas.
- (4) To identify the model parameters, Matlab/Simulink and numerical calculation are utilized to solve the nonlinear formulas according to the cost function with an initial guess and a rational value range of the model parameters,
- (5) In order to ensure the convergence stability and convergence rate, GA is employed in the process of iterative calculation to identify model parameters of the practical servo-mechanical system.

In this way, the linear dynamic model parameters, the minimal level of the Coulomb friction and force ripple can be determined. In light of these results, the measure of the control strategy with feed-forward of friction and force ripple can be taken to improve the tracking performance.

3. Simulations

In this section, to verify the feasibility and identification accuracy, considering a model of servo-mechanism based on (1) to (3), original parameters of the servo-mechanism are assumed and Matlab/Simulink is utilized to carry out the simulation for identifying the model

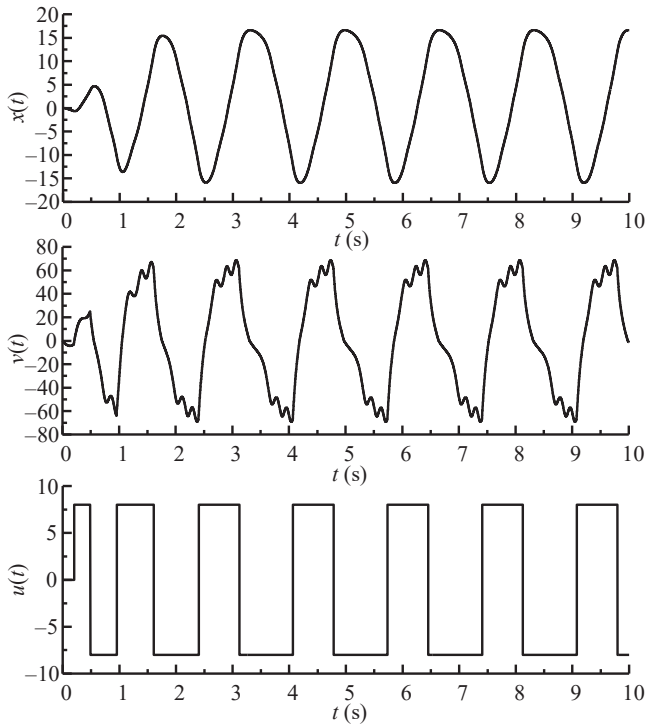


Figure 4. $v(t)$, $x(t)$ and control signal $F(t)$ under the relay gains of (8, 0.2). **Source(s):** Authors' own work

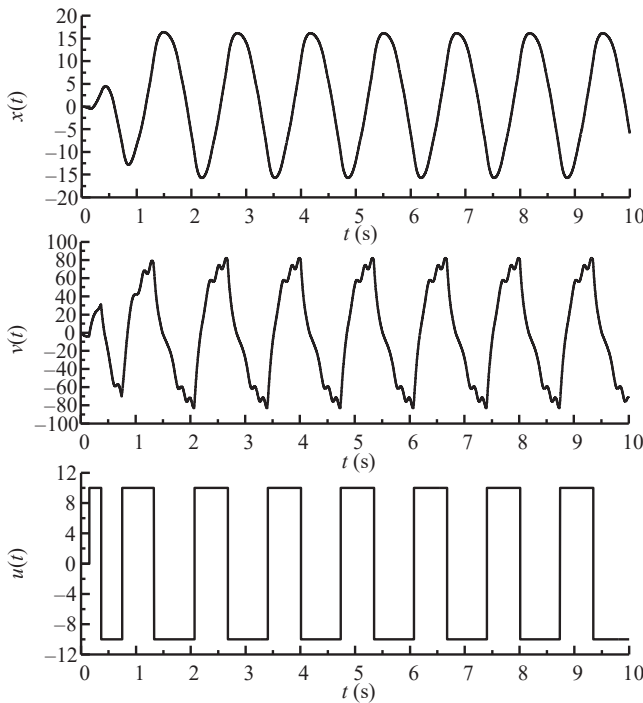


Figure 5. $v(t)$, $x(t)$ and control signal $F(t)$ under the relay gains of (10, 0.15). **Source(s):** Authors’ own work

Table 2. Velocity and position response of oscillation

Serial number	$t(i)$	$v(t)$	$x(t)$	$F(t)$
Relay test with relay gain of (8, 0.2)	2.720	51.886	-10.217	8
	2.910	63.599	-0.629	8
	3.067	68.747	9.217	8
Relay test with relay gains of (10, 0.15)	3.709	58.022	-9.566	10
	3.857	74.324	-0.369	10
	3.988	82.169	9.315	10

Source(s): Authors’ own work

parameters and comparing with the given model. Dynamics of the linear portion, Coulomb friction factor, amplitude and single dominant spatial frequency of the force ripple are set as follows:

$$a = 4, b = 40, C = 3.5, f = 0.4, \Omega = 0.2\pi, \theta = \frac{\pi}{6}$$

For all the following simulations, the sampling time is configured as 0.1 ms.

3.1 Simulation verification

As mentioned previously, in order to identify the model parameters, not only three sampling points of the velocity response in one relay test but also at least two sets of relay experiments

should be taken to establish at least 5 equations. Therefore, relay feedback experiments with various relay parameters (u, D) are performed. Taking the above-mentioned servo model as an example, two sets of relay feedback experiments with relay gains of (10, 0.2) and (15, 0.15) are conducted to excite the oscillations in the nonlinear servo-mechanism. Thus, the output of the relay gain with an artificial delay component is rectangular wave which is the input of the servo-mechanism. Subsequently, the measureable signals of position response, velocity response and relay outputs in the relay feedback are illustrated in [Figures 4 and 5](#).

To acquire the accurate solution of the servo system, GA is applied to the process of iterative calculation. The sampling time and its corresponding velocity and position response of the two sets of relay tests are measured and summarized in [Table 2](#). As shown in [Table 1](#), the sampled points are basically located at the region of velocity fluctuation for exploring the effect of the force ripple on the response of velocity and position.

Afterwards, the model parameters are identified with the following initial guess of $a = 2$, $b = 35$, $C_1 = 0.1$, $C_2 = 0.1$ and $f = 0.1$ and with the variation range of [0, 6], [30, 50], [0, 1], [0, 1] and [0, 1], respectively. Furthermore, as illustrated in [Table 3](#), the amplitude, frequency and offset of the position response in [Figures 4 and 5](#) are 16.295 mm, 2.241 Hz, 4.71 mm and 15.864 mm, 4.71 Hz, 1.35 mm, respectively, which is treated as NPCs in solution process for comparing with TPCs of the intermediate results in the solving process.

On the basis of the proposed numerical solving method, the minimum discrepancy between NPCs and TPCs is searched and specified as the terminate identification results. The terminate identification results under the proposed method is shown in [Table 4](#). Compared with the traditional identification method ([Leea et al., 2015](#)) based on the describe function (DF), the maximum identification error can be kept below 4%, which is a decrease of 7%.

3.2 The effect of various relay parameters on identification results

In order to further explore the relationship between estimation accuracy and various relay parameters, extensive simulation studies are carried out. The relay gain u varies from 7 to 9 with the interval of 0.1, while the dead time D changes from 0 to 0.2 with the interval of 0.01 s. The oscillations are excited for every (u, D) and ($u + 1.0, D$), and the model parameters are solved. Then, the parameter identification results of the proposed method under variable relay

Table 3. NPCs of relay tests with various relay parameters

NPCs (unit)	Relay test with (10, 0.2)	Relay test with (15, 0.15)
Amplitude (mm)	16.295	15.864
Frequency (Hz)	2.241	4.71
Offset (mm)	4.71	1.35

Source(s): Authors' own work

Table 4. Simulation results

Parameters	Actual values	Proposed method	Error %	DF method	Error %
a	4.0	4.0248	0.62	4.0089	0.22
b	40.0	39.668	-0.83	39.4076	-1.48
C_1	1.7500	1.8118	3.53	0.4423	-11.54
C_2	3.0310	3.1110	2.64	0.8810	1.73
f_c	0.4	0.3945	-1.37	0.4107	-2.67

Source(s): Authors' own work

parameters are illustrated in Figure 6. It can be seen that the estimation accuracy of the proposed method can be kept within 8%. Furthermore, an obvious conclusion can be drawn from Figure 6 that the identification accuracy deteriorates as the dead time decreases because the oscillating frequency may be very high and the oscillation amplitude is close to zero, both of which may result in difficulties for measuring the oscillation. In conclusion, the proposed method has a great advantage in robust quality according to the research on the effect of different selections of relay parameters on the estimation accuracy.

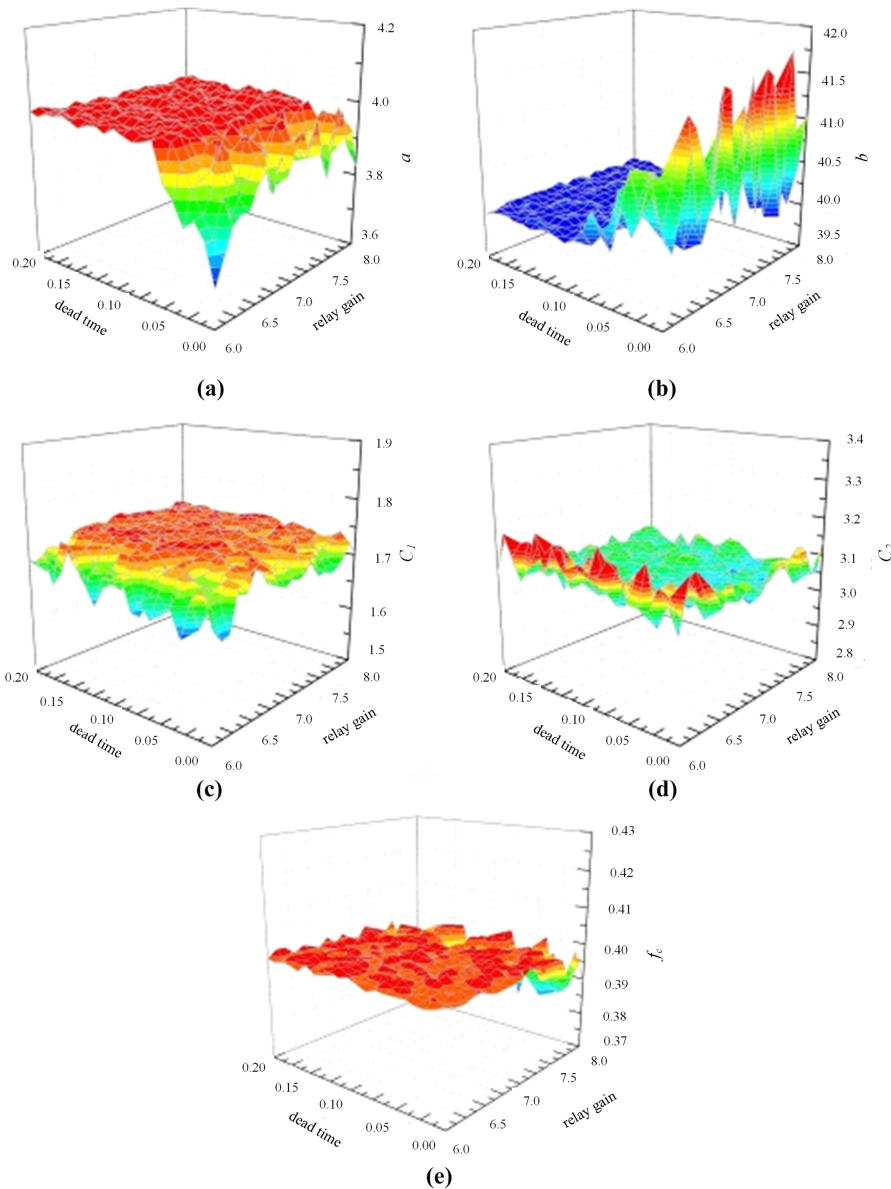


Figure 6. Identification results with various relay parameters. **Source(s):** Authors' own work

4. Real-time experiments

To validate and confirm the correctness of the proposed identification method, real-time experiments are conducted on a platform of direct drive servo-mechanism as shown in Figure 7. The servo-mechanical platform consists of a Beckhoff PLC, a self-developed amplifier based on the EtherCAT bus, as well as a tubular PMSLM driving the load to move

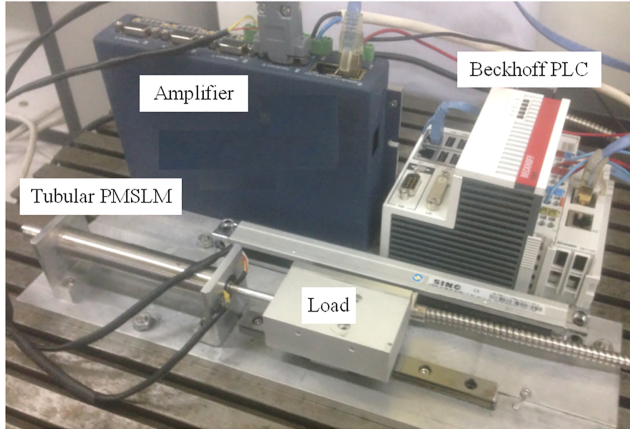


Figure 7. Servo-mechanical system based on a tubular PMSLM. Source(s): Authors' own work

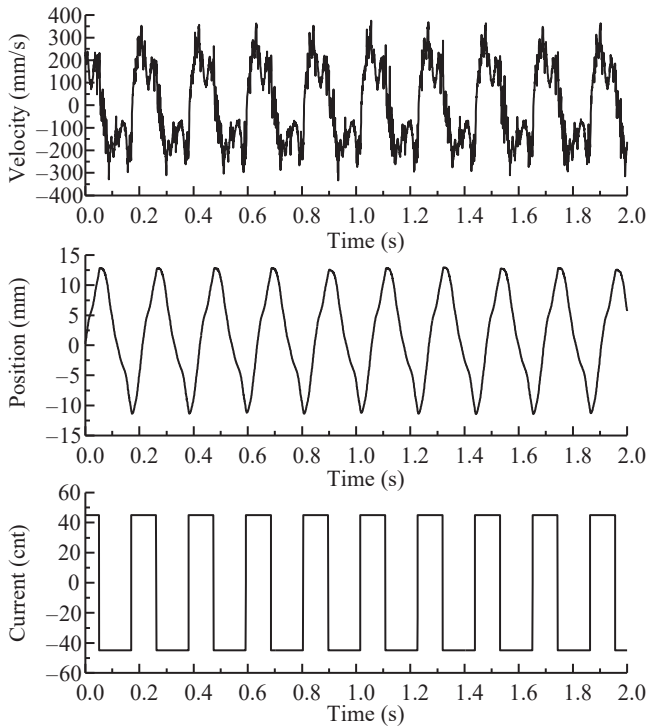


Figure 8. Output $v(t)$, $x(t)$ and control signal $u(t)$ under the relay gains of (45, 0.1). Source(s): Authors' own work

along with the slide rail. Note that the sampling time of the Beckhoff PLC is 0.1 ms and the transducer equipped with the system is a pair of linear hall elements with an effective resolution of 2.5 μm . Accordingly, based on the identification results, a novel control strategy is developed to compare with the tracking performance of the traditional control scheme.

4.1 Servo-mechanism identification

Relay feedback tests are performed with the relay parameters of (45, 0.1) and (50, 0.1), where the value of u can determine the thrust force by converting through the thrust coefficient of the tubular PMSLM. Thus, the oscillation of the nonlinear servo-mechanism can be generated as shown in Figures 8 and 9 and the sampled points are summarized in Table 5. Then, the model

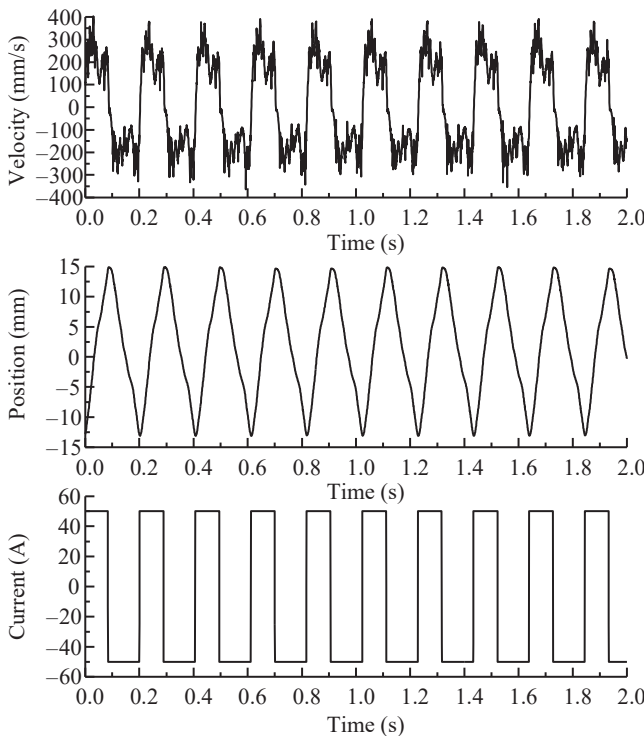


Figure 9. Output $v(t)$, $x(t)$ and control signal $u(t)$ under the relay gains of (50, 0.1). Source(s): Authors' own work

Table 5. Response of oscillations in experiment

Serial number	$t(i)/\text{s}$	$v(t)/\text{mm/s}$	$x(t)/\text{mm}$	$i(t)/\text{mA}$
Relay test with relay gain of (45, 0.2)	0.4199	356.0	-1.179	450
	0.4457	79.2	5.686	450
	0.4595	214.6	8.721	450
Relay test with relay gains of (50, 0.1)	0.6466	392.0	5.149	500
	0.6670	101.3	5.652	500
	0.6808	225.6	8.826	500

Source(s): Authors' own work

parameters can be solved by substituting the sampling points into the nonlinear formulas, according to the solving approach introduced in Section 2.3. Afterwards, the model parameters can be determined as follows: $a = 0.5101$, $b = 15.3047$, $C_1 = 1.72$, $C_2 = 3.34$ and $f = 9.8413e-5$.

To validate the estimation accuracy of the identification results, the identified parameters are substituted into the block in Matlab/Simulink to compare the discrepancy of velocity response between experimental measurement and simulation as shown in Figure 10. As can be observed from Figure 10, the comparison showed a good performance of consistence between simulation and experimental measurement.

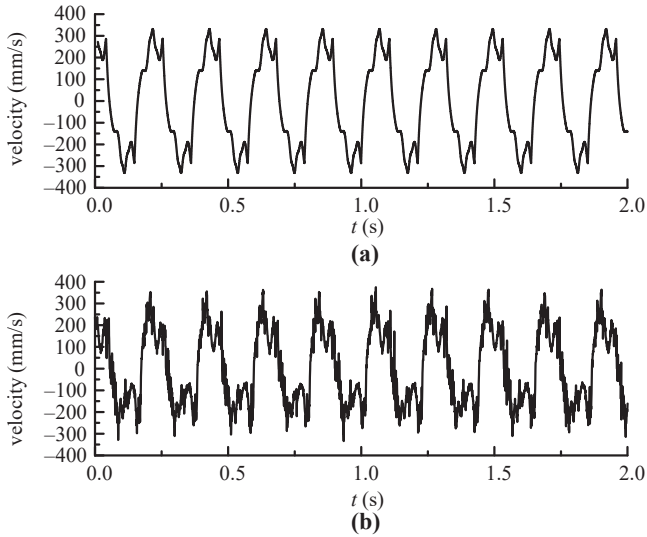


Figure 10. Comparison between (a) simulation results and (b) experiment measurement. **Source(s):** Authors' own work

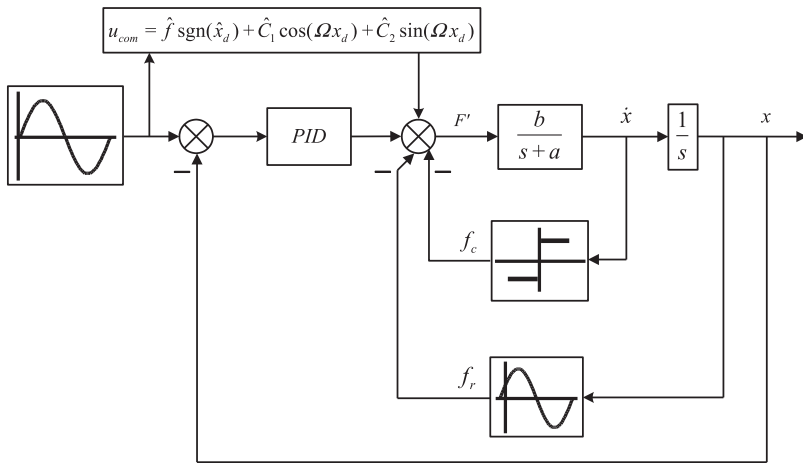


Figure 11. A feed forward control strategy based on identification. **Source(s):** Authors' own work

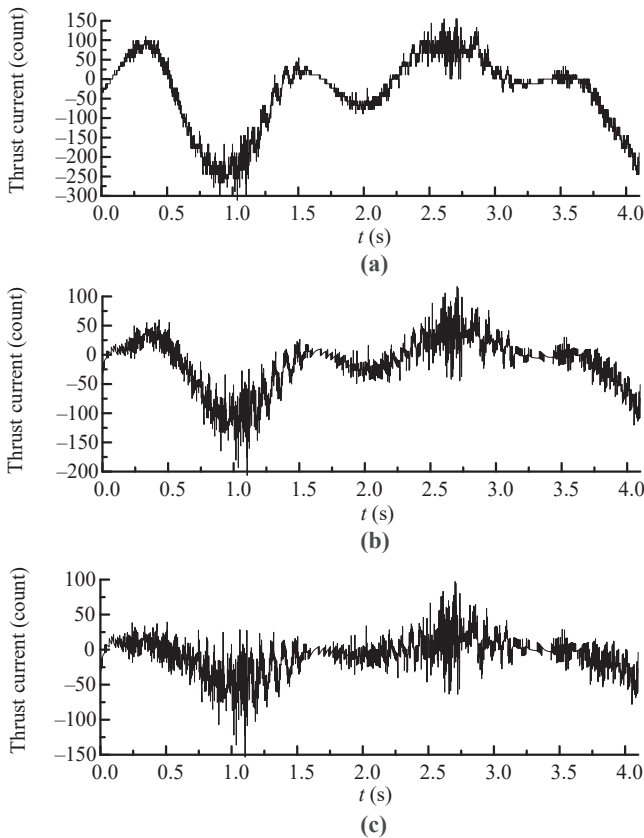


Figure 12. Thrust current in the stage of uniform motion. (a) Without compensation. (b) Compensation based on the DF method. (c) Compensation based on the proposed method. **Source(s):** Authors' own work

4.2 Point-to-point motion

In order to improve the tracking performance, based on a traditional proportional-integral-derivative (PID) controller, Figure 11 illustrated a novel control strategy, on which a feed forward compensator of force ripple and friction is mounted. Particularly, the control parameters of the PID is set as $k_p = 50 \text{ V/mm}$, $k_i = 0$, $k_d = 0.12 \text{ V} \cdot \text{s/mm}$. To investigate the effect of various estimation results on the tracking performance and thrust current, both the identification results of the DF method and the proposed method are taken into the feed-forward compensator.

Firstly, point-to-point position experiment with a constant velocity is employed to check the fluctuation of thrust current and tracking error in the stage of uniform movement. In this experiment, the load moves following a slope curve where the planned velocity and the planned displacement are 5 mm/s and 20 mm , respectively. The results regarding to the thrust current and tracking error are shown in Figures 12 and 13. It can be seen that the fluctuation of the thrust current can be effectively eliminated by the compensation of force ripple and friction. Furthermore, the RMSE can be reduced from $34.1 \mu\text{m}$ to $21.7 \mu\text{m}$ by the DF identification results, while the RMSE can be decreased from $34.1 \mu\text{m}$ to $18.2 \mu\text{m}$ by implementing the results of the proposed method.

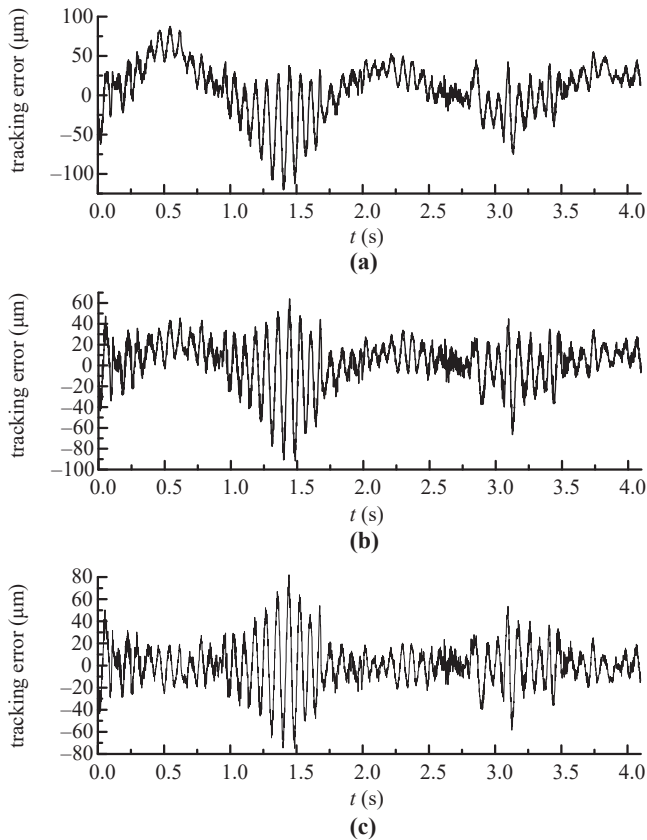


Figure 13. Tracking error in the stage of uniform stage. (a) Without compensation. (b) Compensation based on the DF method. (c) Compensation based on the proposed method. **Source(s):** Authors' own work

4.3 Sinusoid tracking

Sinusoid tracking is also carried out to validate the improvement of tracking performance through the feed-forward compensator. The desired moving profile is set as $x_d = 10\sin(0.5\pi t - 0.5\pi)$ (unit in millimeter), as illustrated in Figure 14(a). Afterwards, Figure 14(b) and Figure 14(c) exhibit the comparative results under the compensator designed by the DF method and the proposed method.

From Figure 14(b), the maximum tracking error is around 148 μm with the compensator designed by the DF method. Figure 14(c) has illustrated the efficiency of the compensator of the proposed method, since the maximum tracking error decreases to 98 μm. Obviously, with the feed-forward compensator, the RMSE of the tracking error can be drastically reduced from 37.96 μm to around 26.00 μm.

5. Conclusions

This paper presents a time-domain relay feedback identification method for characterizing friction nonlinearities and force ripple effects in PMSLMs. The servo-mechanism was mathematically modeled, enabling derivation of its velocity response through first-order system analysis under arbitrary input conditions. Since the oscillation was excited by proper

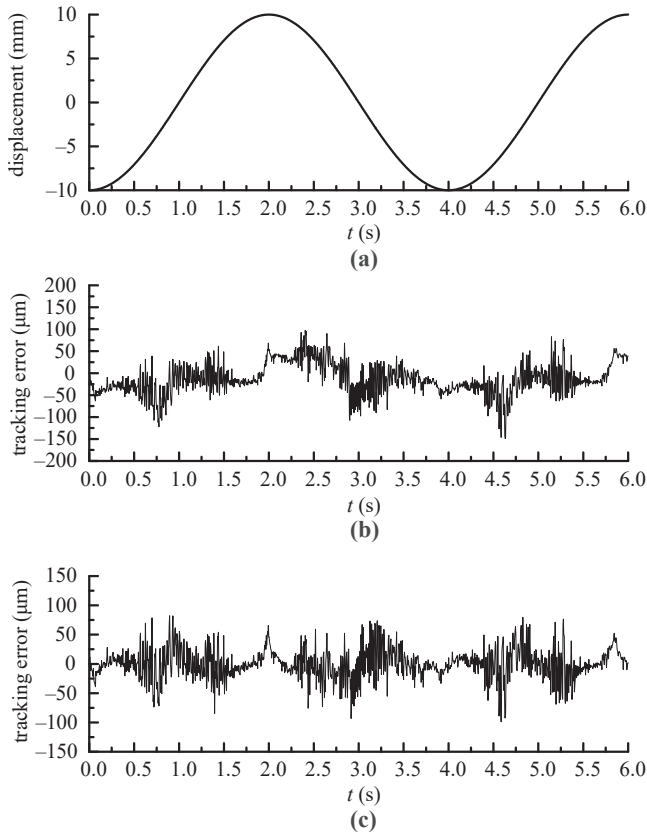


Figure 14. Tracking performance. (a) Without compensation. (b) Compensation based on the DF method. (c) Compensation based on the proposed method. **Source(s):** Authors' own work

relay parameters, the sampling points can be employed to substitute into the above equations. Subsequently, the parameter identification cost function was formulated based on the deviation between NPCs and TPCs. In order to verify the feasibility of the approach, simulations have been employed, and the identified results have shown that the estimation error stays within 8% under various relay parameters. To validate the practicability of the method, a feed-forward compensator based on the identified results was integrated into a traditional PID controller. The maximum tracking error of the sinusoid tracking was reduced from 148 μm to less than 98 μm under the condition that the transducer was a pair of linear hall elements with an effective resolution of 2.5 μm . In conclusion, this novel identification approach can be utilized in different process control and servo-control systems. Moreover, parameter auto-tuning, feed-forward compensation or disturbance observer can be investigated based on the obtained information to improve the system stability and control accuracy.

In the field of rail transit, PMSLM technology can be used in the future electro-mechanical braking system, electro-mechanical sand spraying device, door system and other equipment using motors, which is of great significance to the full electrification of rail transit trains.

Acknowledgments

The authors wish to thank Locomotive and Car Research Institute of China Academy of Railway Sciences Corporation Limited, Beijing Zongheng Electro-Mechanical Technology Co., Ltd., CRRC Changchun

Railway Vehicles Co., Ltd., CRCC Tangshan Co., Ltd. and all team members who participated in the project. This research is sponsored by the National Key R&D Program of China-2022YFB4301203, as well as the Science Foundation of China Academy of Railway Science (No. 2023YJ341).

References

- Ahandani, M. A., Abbasfam, J., & Kharrati, H. (2022). Parameter identification of permanent magnet synchronous motors using quasi-opposition-based particle swarm optimization and hybrid chaotic particle swarm optimization algorithms. *Applied Intelligence: The International Journal of Artificial Intelligence, Neural Networks, and Complex Problem-Solving Technologies*, 52(11), 13082–13096. doi: [10.1007/s10489-022-03223-x](https://doi.org/10.1007/s10489-022-03223-x).
- Ahmad, Z., Hassan, A., Khan, F., & Lazoglu, I. (2020). Design of a high thrust density moving magnet linear actuator with magnetic flux bridge. *IET Electric Power Applications*, 14(7), 1256–1262. doi: [10.1049/iet-epa.2019.0789](https://doi.org/10.1049/iet-epa.2019.0789).
- Astrom, K. J., & Haggglund, T. (1984). A frequency domain method for automatic tuning of simple feedback loops. *IEEE*, 299–304. doi: [10.1109/cdc.1984.272361](https://doi.org/10.1109/cdc.1984.272361).
- Chen, X., Fang, F., & Luo, X. (2014). A friction identification approach based on dual-relay feedback configuration with application to an inertially stabilized platform. *Mechatronics*, 24(8), 1120–1131. doi: [10.1016/j.mechatronics.2014.08.002](https://doi.org/10.1016/j.mechatronics.2014.08.002).
- Chen, F., Chen, Z., Chen, Q., Gao, T., Dai, M., Zhang, X., & Sun, L. (2024). Research on motor rotation anomaly detection based on improved VMD algorithm. *Railway Sciences*, 3(1), 18–31. doi: [10.1108/RS-12-2023-0047](https://doi.org/10.1108/RS-12-2023-0047).
- Dong, H., Chen, F., Wang, Z., Jia, L., & Man, J. (2020). An adaptive multi-sensor fault diagnosis method for high-speed train traction converters. *IEEE Transactions on Power Electronics*, 36(99), 1. doi: [10.1109/TPEL.2020.3034190](https://doi.org/10.1109/TPEL.2020.3034190).
- Hofreiter, M., Mouka, M., & Trnka, P. (2023). Self-tuning controller using shifting method. *Mathematics*, 11(21), 4548. doi: [10.3390/math11214548](https://doi.org/10.3390/math11214548).
- Kadhim, A. A., Rostami, N., & Sharifian, M. B. B. (2024). Development and design of magnetic structures for improving reliability linear motors. *Metallurgical and Materials Engineering*, 30(4), 13. doi: [10.56801/MME1192](https://doi.org/10.56801/MME1192).
- Leea, T., Tana, K. K., Limb, S., & Doua, H. (2015). Iterative learning control of permanent magnet linear motor with relay automatic tuning. Available from: <http://www.semanticscholar.org/paper/23e78d67810af57326157f0f4c4037f804ec938a>
- Li, Z., Zhang, Z. H., Wang, J. S., Wang, K. T., Guo, X. Q., Fan, D. H., & Sun, H. X. (2023). Compensator design of permanent magnet synchronous linear motor control system based on load disturbance observer. *Journal of Electrical Engineering and Technology*, 18(5), 12–3720. doi: [10.1007/s42835-023-01465-4](https://doi.org/10.1007/s42835-023-01465-4).
- Liu, C., Yao, J., & Jia, Y. (2024). Vehicle height control based on active suspension with permanent magnet synchronous linear motor. *Proceedings of the Institution of Mechanical Engineers, Part D: Journal of Automobile Engineering*, 238(5), 1191–1200. doi: [10.1177/09544070221141495](https://doi.org/10.1177/09544070221141495).
- Liu, X., Wang, H., Zhao, Z., Yang, C., Jia, W., Ji, Y., & Qiu, H. (2025). Analysis of vibration reduction of single-side permanent magnet synchronous linear motor by using hybrid-type PMs. *IEEE Transactions on Transportation Electrification*, 11(1), 2877–2885. doi: [10.1109/TTE.2024.3422988](https://doi.org/10.1109/TTE.2024.3422988).
- Pal, A., & Mudi, R. (2022). Speed control of DC motor using relay feedback tuned PI, fuzzy PI and self-tuned fuzzy PI controller. Available from: <http://doc.paperpass.com/foreign/rgArti0000154768841.html>
- Pang, Y., Yu, H., Wang, M. Y., Zhicheng, Y., Ali, M., & Ye, Z. (2023). Non-cascaded finite time control of PMSLM based on super-twisting observer. *International Journal of Applied Electromagnetics and Mechanics*, 73(3), 175–190. doi: [10.3233/JAE-220200](https://doi.org/10.3233/JAE-220200).
- Qiao, L., Du, J., Wang, Y., & Yang, Z. (2023). Thrust fluctuation suppression of PMSLM considering flux linkage harmonics and cogging force. In *2023 26th International Conference on Electrical Machines and Systems (ICEMS)* (pp. 416–420). doi: [10.1109/icems59686.2023.10345148](https://doi.org/10.1109/icems59686.2023.10345148). Available from: <http://ieeexplore.ieee.org/document/10345148/>

- Rehan, A., Boiko, I., & Zweiri, Y. (2024). Autotuning of PID controller using the modified relay feedback test and optimization under uncertainty principle for robotic manipulators. *IET Control Theory and Applications (Wiley-Blackwell)*, 18(5), 581–602. doi: [10.1049/cth2.12592](https://doi.org/10.1049/cth2.12592).
- Rigatos, G., Zervos, N., Abbaszadeh, M., Siano, P., & Siadimas, V. (2020). Neural networks and statistical decision making for fault diagnosis of PM linear synchronous machines. *International Journal of Systems Science*, 51(3), 1–17. doi: [10.1080/00207721.2020.1792579](https://doi.org/10.1080/00207721.2020.1792579).
- Shi, X., Han, Y., Wu, J., & Liu, C. (2019). Researches on time-domain relay feedback identification approaches for high-acceleration linear servo systems. doi: [10.1007/978-3-030-22868-2_32](https://doi.org/10.1007/978-3-030-22868-2_32).
- Song, C., Xu, B., Fan, X., Yang, P., & Duan, R. (2022). Design, analysis, control simulation, and experiment of novel electromagnetic hybrid vibration absorber. *Proceedings of the Institution of Mechanical Engineers, Part C: Journal of Mechanical Engineering Science*, 236(6), 2740–2755. doi: [10.1177/09544062211035806](https://doi.org/10.1177/09544062211035806).
- Strm, K. J., & Hgglund, T. (1984). Automatic tuning of simple regulators with specifications on phase and amplitude margins. *Automatica*, 20(5), 645–651. doi: [10.1016/0005-1098\(84\)90014-1](https://doi.org/10.1016/0005-1098(84)90014-1).
- Taha, W., & Emadi, A. (2021). Online non-parametric auto-tuning of flux weakening controller for IPMSM drives using modified relay feedback test. In *IEEE Transportation Electrification Conference and Expo* (pp. 309–314). doi: [10.1109/itec51675.2021.9490113](https://doi.org/10.1109/itec51675.2021.9490113). Available from: https://www.zhangqiaokeyan.com/academic-conference-foreign_meeting_thesis/0205117821364.html
- Visioli, A., & Sanchez-Moreno, J. (2024). A relay-feedback automatic tuning methodology of PIDA controllers for high-order processes. *International Journal of Control*, 97(1/3), 51–58. doi: [10.1080/00207179.2022.2135019](https://doi.org/10.1080/00207179.2022.2135019).
- Wang, C., & Wang, A. (2023). Research on parameter identification algorithm of permanent magnet synchronous motor considering dead time compensation. *Progress in Electromagnetics Research C*, 138, 205–218. doi: [10.2528/pierc23071402](https://doi.org/10.2528/pierc23071402).
- Wang, S., Liu, C., Wang, Y., Lei, G., Guo, Y., & Zhu, J. (2020). Electromagnetic performance analysis of flux-switching permanent magnet tubular machine with hybrid cores. *China Electrotechnical Society Transactions on Electrical Machines and Systems*, 4(1), 10–52. doi: [10.30941/cestems.2020.00007](https://doi.org/10.30941/cestems.2020.00007).
- Wang, L., Lv, Q., Wu, F., Zhang, R., & Gao, F. (2024). Non-excitation closed-loop identification based on hysteresis bias relay feedback. *Computers and Chemical Engineering*, 188, 13. doi: [10.1016/j.compchemeng.2024.108776](https://doi.org/10.1016/j.compchemeng.2024.108776).
- Wu, X., Song, J., Duan, Z., Wang, X., Ding, W., Wu, J., & Lu, S. (2024). Air gap flux density measurement of PMSLM based on TMR sensing external stray magnetic field and CNN-LSTM. *Measurement*, 231, 114617. doi: [10.1016/j.measurement.2024.114617](https://doi.org/10.1016/j.measurement.2024.114617).
- Yang, R., Li, L., Wang, M., & Zhang, C. (2021). Force ripple compensation and robust predictive current control of PMSM using augmented generalized proportional–integral observer. *IEEE*, 9(1), 302–315. doi: [10.1109/jestpe.2019.2938268](https://doi.org/10.1109/jestpe.2019.2938268).
- Ye, Y., Cai, D., Geng, L., Yan, H., Yao, J., & Chen, F. (2022). A constitutive model for cyclic densification of coarse-grained soil filler for the high-speed railway subgrade considering particle breakage. *Railway Sciences*, 1(1), 1–15. doi: [10.1108/RS-04-2022-0020](https://doi.org/10.1108/RS-04-2022-0020).
- Zhao, F., Liu, J., Zhang, C., Zhao, Z., Ning, X., & Wang, J. (2025). Current development and prospect of national science and technology innovation platform in the railway industry. *Railway Sciences*, 4(2), 266–279. doi: [10.1108/RS-12-2024-0055](https://doi.org/10.1108/RS-12-2024-0055).
- Zhou, M., Hao, Q., Zou, W., & Liu, Z. (2024). Adaptive servo system parameter tuning with success-driven differential evolution. In *International Conference on Computing, Control and Industrial Engineering* (pp. 106–116). doi: [10.1007/978-981-97-6934-6_14](https://doi.org/10.1007/978-981-97-6934-6_14).



Fuzhao Chen received his Master's degree in Control Science and Engineering from Beijing Jiaotong University. He currently serves as an assistant researcher at the Locomotive & Car Research Institute of the China Academy of Railway Sciences. He is engaged in scientific research on train braking systems, and the train braking systems he has participated in developing have been widely applied.

Corresponding author

Fuzhao Chen can be contacted at: fzchen001@163.com

For instructions on how to order reprints of this article, please visit our website:

www.emeraldgroupublishing.com/licensing/reprints.htm

Or contact us for further details: permissions@emeraldinsight.com